Title: Multistate and Multistage Synchronization of Hindmarsh-Rose Neurons With Excitatory Chemical and Electrical Synapses

標題: 刺激性化學與電子耦合的 Hindmarsh-Rose 神經細胞其產生的多狀態、層級同步現象

Abstract: The new phenomena of the multistate synchronization of Hindmarsh-Rose (HR) neurons with both excitatory chemical and electrical synapses over the complex network are analytically studied. The regions for coupling strengths to achieve local synchronization are explicitly obtained. Such regions are characterized by the second largest eigenvalue λ_2 of the electrical connection matrix and the number k of chemical signals each neuron receives. The dynamics of the multistate synchronization includes the coexistence of stable regular bursting and periodic/ steady-state behaviors. Our theory predicts that recurrent networks formed by a certain cell types in layers 4 and 6 in cat area 17 could lead to multistate synchronization. These are in contrast with coupled oscillator systems or coupled map lattices where only single-state synchronization is found. It should also be noted that if the parameters of HR neurons are chosen resulting in an irregular (chaotic) bursting, then the coexistence state would contain chaotic attractor. Our method employed here is quite general. For instance, it can be immediately applied to other coupled nervous systems such as FitzHugh-Nagumo and Morris-Lecar nervous systems. The analytical tools and concepts needed include coordinate transformations, matrix measures, monotone dynamics and time averaging estimates.

摘要: 本文用分析的方法研究刺激性的化學與電子耦合的 Hindmarsh-Rose (HR) 神經細胞產生的多狀態同步的神經網絡。達成局部同步的耦合強度的區域可以明確地求出。這個區域與電子連結矩陣的第二大特徵值λ_2及每個神經細胞接收到的化學信號數量k有關。多狀態同步的動態包括穩定規律爆發以及週期/穩態行為的共存。我們對於在貓的區域17中階層4和階層6的細胞類型形成的遞迴網路的理論預測可以達到多狀態同步。這些和僅能發現單一狀態同步的耦合振盪器系統或是網格形耦合映射形成對比。我們也注意到，如果在HR神經細胞裡選擇了會產生不規則(混沌)爆發的參數，則混沌吸引子也會在共存狀態中。我們的方法很一般。我們的方法很一般，例如，它可以立即應用到其他單神經元模型，如 FitzHugh-Nagumo 模型。所需的工具和概念，包括坐標變換，矩陣測度，單調動力學和時間平均估計。

Multistate and Multistage Synchronization of Hindmarsh-Rose Neurons With Excitatory Chemical and Electrical Synapses

Fang-Jhu Jhou, Jonq Juang, and Yu-Hao Liang

Abstract—The new phenomena of the multistate synchronization of Hindmarsh-Rose (HR) neurons with both excitatory chemical and electrical synapses over the complex network are analytically studied. The regions for coupling strengths to achieve local synchronization are explicitly obtained. Such regions are characterized by the second largest eigenvalue λ_2 of the electrical connection matrix and the number k of chemical signals each neuron receives. The dynamics of the multistate synchronization includes the coexistence of stable regular bursting and periodic/steady-state behaviors. Our theory predicts that recurrent networks formed by a certain cell types in layers 4 and 6 in cat area 17 could lead to multistate synchronization. These are in contrast with coupled oscillator systems or coupled map lattices where only single-state synchronization is found. It should also be noted that if the parameters of HR neurons are chosen resulting in an irregular (chaotic) bursting, then the coexistence state would contain chaotic attractor. Our method employed here is quite general. For instance, it can be immediately applied to other coupled nervous systems such as FitzHugh-Nagumo and Morris-Lecar nervous systems. The analytical tools and concepts needed include coordinate transformations, matrix measures, monotone dynamics and time averaging estimates.

Index Terms—Chemical and electrical synapses, Hindmarsh-Rose neurons, multistate synchronization.

I. INTRODUCTION

THE fundamental building block of every nervous system is the neuron. There is an increasing trend [1]–[3] towards studying the dynamical behavior of relatively large networks of neurons, and modeling/emulating such networks is also on the rise. Neural synchronization has been suggested as particularly relevant for neuronal signal transmission and coding in the brain. Brain [4]–[11] oscillations that are ubiquitous phenomena in all brain areas eventually get into synchrony and con-

sequently allow the brain to process various tasks from cognitive to motor tasks. Indeed, it is hypothesized that synchronous brain activity is the most likely mechanism for many cognitive functions such as attention, feature binding, learning, development, and memory function. In this paper, the new phenomena of the multistate and multistage synchronization of Hindmarsh-Rose neurons with excitatory chemical and electrical synapses over the complex network are analytical studied.

In the last decades, many biological neuron models have been proposed for an accurate description and prediction of biological phenomena. The pioneering work in such direction is due to Hodgkin and Huxley. To simplify such a model, simpler approximations, namely, the second order systems such as the FitzHugh-Nagumo (FN) and Morris-Lecar neuron models have been proposed. However, the second order models are not able to reproduce some interesting phenomena such as terminating themselves by triggering a set of stable firings. Hence, the Hindmarsh-Rose (HR) model was added a third dynamical component, whose role is to tune the above subsystem over the mono- and bistability regions in order to activate or terminate the neuronal response. The third order system of HR has turned out to be accurate in capturing both qualitative and quantitative aspects of experimental data [12]–[15]. Furthermore, major neuronal behaviors such as spiking, bursting, and chaotic regime have been produced by such HR model [15]–[17].

In a human brain, there are about 10^{10} neurons with an approximate 10^{14} links between them. Neurons are sparsely connected and their underlying network has small-world property [10] though they are within only a few synaptic steps from other neurons. Neurons in a population synchronize their activity using electrical and chemical synapses with other neurons in the same population as well as with neurons from other populations. Note that the electrical coupling via gap junctions is linear and directly depends on the difference of the membrane potentials. And the chemical coupling is pulsatile and often modeled as a static sigmoidal nonlinear input-output function with a threshold and saturation.

In this work, we study the multistate and multistage synchronization in ensembles of electrically and chemically coupled HR neurons whose connection topology with respect to the electrical coupling is allowed to be complex including, e.g., Newman-Wattts networks, and whose coupling through chemical synapse is unidirectional from presynaptic cell to the postsynaptic cell. By *multistate synchronization*, we mean that given a fixed set of parameters, the corresponding system is capable of producing the coexistence of stable regular bursting and pe-

F.-J. Jhou is with the Department of Mathematical and Scientific Computing, National Chiao Tung University, Hsinchu 300, Taiwan (e-mail: la1110.imm97g@nctu.edu.tw).

J. Juang is with the Department of Applied Mathematics, and Center of Mathematics Modeling and Scientific Computing, National Chiao Tung University, Hsinchu 300, Taiwan, and the National Center for Theoretical Sciences, Hsinchu 300, Taiwan (e-mail: jjuang@math.nctu.edu.tw).

Y.-H. Liang is with the Department of Applied Mathematics, National Chiao Tung University, Hsinchu 300, Taiwan (e-mail: moonsea.am96g@g2.nctu.edu.tw).

riodic/steady-state synchronization, depending on the choice of initial conditions. By varying certain parameters, if the associated system is capable of yielding different types of synchronization such as chaotic, periodic, or steady-state synchronization, then the system is said to exhibit the *multistage synchronization*. Our main results contain the following. The regions in terms of chemically and electrically coupling strengths for local stability of the completely synchronous state in complex networks of HR neurons are explicitly obtained. They depend on the details of the topology of the electrically connected network, the second largest eigenvalue of its associated connection matrix. However, only the number of chemical signals each neuron receives is relevant in obtaining the regions. Moreover, with the presence of both chemical and electrical synapses in the network, the exhibition of multistate synchronization is provided. Our theory predicts that recurrent networks formed by a certain cell types in layers 4 and 6 in cat area 17 could lead to multistate synchronization. This is in contrast with coupled oscillator systems or coupled map lattices where only single-state synchronization is observed. Since on the synchronous manifold, the dynamics of the synchronous equation goes from regular bursting to periodic (spiking) to steady-state as one varies the parameter kg_s. Consequently, the phenomenon of the multistage synchronization is also observed. Furthermore, the following information concerning synchronization of the system can be extracted. First, it is shown that even without the electrical coupling, the coupled neurons may reach stable steady-state synchrony regardless of how sparsely the chemically coupling network is coupled and that the minimum chemically coupling strength is inversely proportional to the number of chemical signals each neuron receives. If, in addition, the network is also electrically coupled, then the minimum electrically coupling strength to reach stable regular bursting synchronization or multistate synchronization can also be explicitly computed. Second, we provide a measurement of how densely coupled the system should be so as to have the chemical synapses playing a positive effect on achieving the synchrony of the system. Our method employed here is quite general. For example, it can be immediately applied to other single neuron models such as the FitzHugh-Nagumo and Morris-Lecar models. The analytical tools and concepts needed include coordinate transformations, matrix measures, monotone dynamics, and time averaging estimates.

The most closely related works to ours are those done by Jalili [18], Kopell and Ermentrout [19], Belykh, Lange, and Hasler [20], Checco, Righero, Biey, and Kocarev [21] and Wang etc., [22]–[24]. In [19], the single neuron model is a quadratic integrate and fire. They obtained that the chemical and electrical couplings play complementary roles in the coherence of rhythms in inhibitory networks. In [20], densely coupled HR system with only chemical coupling was studied. They demonstrated the bound of the minimum chemical strength for obtaining the steady-state synchronization only depends on the number of signals each neuron receives, independent of all other details of the network topology. These two works used both numerical and analytical techniques to address local synchronization. Coupled HR system with only chemical coupling was also investigated in [21]. They have found multistage synchroniza-

tion. However, the presence of multistate synchronization has not been addressed there. Furthermore, their results are based on the Master Stability Equation, which is numerical in nature, whereas the results in [18], though the same model as ours were studied, was numerical. The surprising new phenomenon of multistate synchronization was not mentioned there. The work done in [22]–[24] dealt with only electrical coupling. However, effects of delay on synchronization were investigated there, where some interesting results are obtained when delays are varied.

The paper is organized as follows. Section II is to lay down the foundation of our paper. Some needed preliminaries, including coordinate transformations and matrix measures are recorded in the Appendix. The analysis leading to the main result is recorded in Section III. The main results are contained in Section IV. Some comparisons with existing methods are addressed in the end of the section. Some concluding remarks are provided in Section IV.

II. FORMULATION

The HR model was obtained by biological consideration over the response to stimuli of a real neuronal cell. The motion of the model reads as follows:

$$
\begin{aligned}
\dot{x} &= f(x) + y - z + q, \\
\dot{y} &= -y - 5x^2 + 1, \\
\dot{z} &= \mu(b(x - x_0) - z).
\end{aligned}
\tag{1}
$$

Here $f(x) = ax^2 - x^3$, x is the membrane potential, y and z are the recovery (fast) and the adaptation (slow) current, respectively. The roles played by the system parameters are roughly the following. q mimics the membrane input current for biological neurons; a allows one to switch between bursting and spiking behaviors and to control the spiking frequency; μ controls the speed of variation of the slow variable z and in the presence of spiking behaviors, it governs the spiking frequency, whereas in the case of bursting, it affects the number of spikes per burst; b governs adaptation; a unitary value of b determines spiking behavior without accommodation and subthreshold adaptation, whereas around $b = 4$ give strong accommodation and subthreshold overshoot, or even oscillations; x_0 sets the resting potential of the system. Hereafter, the parameters are chosen and fixed as follows: $x_0 = -1.6$, $\mu = 0.01$, $b = 4$, $q = 4$, and $a = 2.6$. The dynamics of the neuron with such set of parameters is regular bursting (see, e.g., [14]). Moreover, the dynamics on the corresponding synchronous manifold of the coupled HR neurons may generate multistability region (see (5) and Table I) containing a stable regular bursting, a stable periodic solution and a stable fixed point.

Neuronal synaptic connections are either chemical or electrical, and chemical connections might be excitatory or inhibitory. Moreover, the electrical coupling through gap junctions is bidirectional, whereas the chemical synapse is unidirectional from the presynaptic cell to the postsynaptic cell. In fact, the current q_{ij} injected from the presynaptic cell j to the postsynaptic cell i, is a nonlinear function of the membrane potential x_j of the presynaptic cell and a linear function of the

TABLE I
THE DYNAMICS OF SYNCHRONOUS EQUATION (5) WITH VARIOUS RANGE OF kg_s. THE MULTISTABILITY OF (5) IS OBSERVED WITH $kg_s \in [0.809, 0.85]$

kg_s	$kg_s < 0.808$	$0.809 \le kg_s \le 0.813$	$0.814 \le kg_s \le 0.85$	$kg_s \ge 0.87$
Types	Stable regular bursting	Stable regular bursting	Stable regular bursting	Stable steady state
		Stable periodic solution	Stable steady state	

membrane potential x_i of the postsynaptic cell. The current q_{ij} has the following form:

$$q_{ij} = g_s(v - x_i)p(x_j), \tag{2a}$$

where g_s is the strength of chemical coupling and v is the synaptic reversal potential. If $x_i < v$, the current injected to the cell is positive and depolarizes it, thus the coupling is excitatory. On the other hand, for $x_i > v$, the injected current to the cell is negative and consequently hyperpolarizes it, thus introducing inhibitory coupling. In this paper, we numerically choose $v = 2$ so that $x_i(t) < v$ for all t, thus the synapse is depolarizing (excitatory). It is certainly interesting to justify that such choice of v is always possible.

The chemically synaptic coupling function is modeled by the sigmoidal function

$$p(x_j) = \frac{1}{1 + \exp\{-\lambda(x_j - \theta_s)\}}, \tag{2b}$$

where $\theta_s = -0.25$ is the threshold and $\lambda = 10$. The threshold is chosen so that every spike in the single neuron burst can reach the threshold. In the limit $\lambda \to \infty$, the above sigmoid function reduces to a Heaviside step function.

We are now in a position to consider a network of n excitatory HR neurons with bidirectional electrical coupling and unidirectional excitatory chemical coupling. The equations of motion are the following. For, $i = 1, \ldots, n$,

$$\dot{x}_i = f(x_i) + y_i - z_i + q + \sigma \sum_{j=1}^{n} g_{ij}x_j$$
$$- g_s(x_i - v)\sum_{j=1}^{n} c_{ij}p(x_j)$$
$$= f(x_i) + y_i - z_i + q + \sigma \sum_{j=1}^{n} g_{ij}x_j$$
$$- g_s k(x_i - v)p(x_i) - g_s(x_i - v)\sum_{j=1}^{n} d_{ij}p(x_j),$$
$$\dot{y}_i = -y_i - 5x_i^2 + 1,$$
$$\dot{z}_i = \mu(b(x_i - x_0) - z_i), \tag{3}$$

where

$$\mathbf{G} =: (g_{ij}), \sum_{j=1}^{n} g_{ij} = 0 \text{ for all } i, \tag{4a}$$

$$\mathbf{C} =: (c_{ij}), \ c_{ij} = 0 \text{ or } 1,$$

$$c_{ii} = 0, \sum_{j=1}^{n} c_{ij} = k \text{ for all } i, \tag{4b}$$

and

$$\mathbf{D} =: (d_{ij}), \text{ and } d_{ij} = \begin{cases} -k & \text{if } i = j, \\ c_{ij} & \text{if } i \ne j. \end{cases} \tag{4c}$$

Here k represents the number of chemical signals each neuron receives. Moreover, σ is the coupling strength for electrical synapses via gap junctions, and coupling matrix $\mathbf{G}$ is a symmetric matrix with vanishing row sums and nonnegative off-diagonal entries. It should be noted that the symmetry of $\mathbf{G}$ is a biological assumption. From the mathematical side, our analysis here is capable of treating unsymmetrical matrices with both positive and negative off-diagonal entries. $\mathbf{C}$ is the connection matrix of the chemical coupling which is not necessarily symmetric; $c_{ij} = 1$ if neuron i receives synaptic current (via chemical synapses) from neuron j, otherwise $c_{ij} = 0$. The matrix $\mathbf{D}$ has all row sums being zero and nonnegative off-diagonal entries.

We next describe the synchronous equation of HR network (3). On the synchronous manifold, its dynamics is governed by the following equations:

$$\dot{x} = f(x) + y - z + q - kg_s(x - v)p(x),$$
$$\dot{y} = -y - 5x^2 + 1,$$
$$\dot{z} = \mu(b(x - x_0) - z). \tag{5}$$

To study local synchronization, we begin with the derivation of the variational equation of (3) along the synchronous manifold $x_i(t) = x(t)$, $y_i(t) = y(t)$, and $z_i(t) = z(t)$, $i = 1, \ldots, n$. The equation is

$$\dot{u}_i = f'(x(t))u_i + v_i - w_i + \left[\sigma \sum_{j=1}^{n} g_{ij}u_j\right] - kg_s p(x(t))u_i$$
$$- \left[g_s(x(t) - v)p'(x(t))\sum_{j=1}^{n} c_{ij}u_j\right],$$
$$\dot{v}_i = -v_i - 10x(t)u_i,$$
$$\dot{w}_i = \mu(bu_i - w_i), \tag{6}$$

where $x(t)$ lies on the synchronous manifold of (3) and satisfies equation (5).

In vector-matrix form, (6) becomes

$$\dot{\mathbf{u}} = \{[f'(x(t)) - kg_s p(x(t))]\mathbf{I} + \sigma\mathbf{G}$$
$$- g_s(x(t) - v)p'(x(t))\mathbf{C}\}\mathbf{u} + \mathbf{v} - \mathbf{w}$$
$$= \{[f'(x(t)) - kg_s p(x(t)) - kg_s(x(t) - v)p'(x(t))]\mathbf{I}$$
$$+ \sigma\mathbf{G} - g_s(x(t) - v)p'(x(t))\mathbf{D}\}\mathbf{u} + \mathbf{v} - \mathbf{w}, \tag{7a}$$
$$\dot{\mathbf{v}} = -10x(t)\mathbf{u} - \mathbf{v}, \tag{7b}$$
$$\dot{\mathbf{w}} = \mu b\mathbf{u} - \mu\mathbf{w}. \tag{7c}$$

To study synchronized HR neurons (3), we first apply a coordinate transformation on $\mathbf{G}$ so that the synchronous manifold is isolated and the resulting matrix has a negative matrix measure as possible. The structure of linear system (7a)–(7c) is then explored so that the theory of some monotone dynamics and time averaging estimates can be applied to make the linear system asymptotically stable. Such approach is recorded in the following section.

III. MATHEMATICAL TOOLS

To keep the technical parts of the paper minimum, all the needed propositions to prove Theorem 1 of this section are briefly indicated in the appendix.

To isolate the synchronous manifold, we consider the following class of coordination transformations, which is originated in [25]. Let

$$\mathfrak{C} = \{\mathbf{E} \in \mathbb{R}^{(n-1)\times n} : \mathbf{E} \text{ is of full rank,}$$
$$\text{and all its row sums are zeros}\}$$

and $\mathfrak{D} \subset \mathfrak{C}$ be such that

$$\mathfrak{D} = \left\{ \mathbf{E} \in \mathfrak{C} : \begin{pmatrix} \mathbf{E} \\ \mathbf{e}^T \end{pmatrix} \text{ is orthogonal} \right\}, \qquad (8a)$$

where $\mathbf{e} = 1/\sqrt{n}(1,1,\ldots,1)^T$. Define

$$\mathbf{A} = \begin{pmatrix} \mathbf{E} \\ \mathbf{e}^T \end{pmatrix}, \qquad (8b)$$

where $\mathbf{E} \in \mathfrak{D}$. Then $\mathbf{A}^{-1} = \mathbf{A}^T = (\mathbf{E}(\mathbf{E}\mathbf{E}^T)^{-1}, \mathbf{e}) =: (\mathbf{E}^\dagger, \mathbf{e})$. For any matrix $\mathbf{G} \in \mathbb{R}^{n\times n}$ whose row sums are all equal to zero, we have that

$$\mathbf{A}\mathbf{G}\mathbf{x} = \mathbf{A}\mathbf{G}\mathbf{A}^{-1}\mathbf{A}\mathbf{x} = \begin{pmatrix} \mathbf{E}\mathbf{G}\mathbf{E}^\dagger & \mathbf{0} \\ * & 0 \end{pmatrix} \mathbf{A}\mathbf{x}$$

$$= \begin{pmatrix} \mathbf{E}\mathbf{G}\mathbf{E}^\dagger & \mathbf{0} \\ * & 0 \end{pmatrix} \begin{pmatrix} \bar{\mathbf{x}} \\ \sum\limits_{i=1}^{n} \frac{x_i}{\sqrt{n}} \end{pmatrix}$$

$$= \begin{pmatrix} \mathbf{E}\mathbf{G}\mathbf{E}^\dagger\bar{\mathbf{x}} \\ *\bar{\mathbf{x}} \end{pmatrix} =: \begin{pmatrix} \bar{\mathbf{G}}\bar{\mathbf{x}} \\ *\bar{\mathbf{x}} \end{pmatrix},$$

where for any given matrix $\mathbf{B}$, we define

$$\bar{\mathbf{B}} = \mathbf{E}\mathbf{B}\mathbf{E}^\dagger. \qquad (8c)$$

Letting

$$\bar{\mathbf{x}} = \mathbf{A}\begin{pmatrix} u_1 \\ \vdots \\ u_n \end{pmatrix}, \bar{\mathbf{y}} = \mathbf{A}\begin{pmatrix} v_1 \\ \vdots \\ v_n \end{pmatrix}, \bar{\mathbf{z}} = \mathbf{A}\begin{pmatrix} w_1 \\ \vdots \\ w_n \end{pmatrix},$$

and multiplying $\mathbf{A}$ on both sides of (7a), we get

$$\dot{\bar{\mathbf{x}}} = [f'(x(t)) - kg_s p(x(t)) - kg_s(x(t) - v)p'(x(t))]\,\bar{\mathbf{x}}$$
$$+ \sigma \begin{pmatrix} \bar{\mathbf{G}} \\ * \end{pmatrix} \bar{\mathbf{x}} + g_s(v - x(t))p'(x(t)) \begin{pmatrix} \bar{\mathbf{D}} \\ * \end{pmatrix} \bar{\mathbf{x}} + \bar{\mathbf{y}} - \bar{\mathbf{z}}.$$

Let $\bar{\mathbf{x}} = (\bar{x}_1, \ldots, \bar{x}_n)^T$. Set $\tilde{\mathbf{x}} = (\bar{x}_1, \ldots, \bar{x}_{n-1})^T$. We have that the dynamics of $\tilde{\mathbf{x}}$ is now satisfied by the following equation:

$$\dot{\tilde{\mathbf{x}}} = \{[f'(x(t)) - kg_s p(x(t)) - kg_s(x(t) - v)p'(x(t))]\,\mathbf{I}$$
$$+ \sigma\bar{\mathbf{G}} + g_s(v - x(t))p'(x(t))\bar{\mathbf{D}}\}\tilde{\mathbf{x}} + \tilde{\mathbf{y}} - \tilde{\mathbf{z}}$$
$$:= \tilde{\mathbf{H}}(t)\tilde{\mathbf{x}} + \tilde{\mathbf{y}} - \tilde{\mathbf{z}}. \qquad (9a)$$

Let $\tilde{\mathbf{y}}$ and $\tilde{\mathbf{z}}$ be similarly defined. Then their motions of dynamics read

$$\dot{\tilde{\mathbf{y}}} = -10x(t)\tilde{\mathbf{x}} - \tilde{\mathbf{y}}, \qquad (9b)$$

and

$$\dot{\tilde{\mathbf{z}}} = \mu b\tilde{\mathbf{x}} - \mu\tilde{\mathbf{z}}. \qquad (9c)$$

Instead of calculating the transverse Lyapunov exponents of the corresponding variational equation (6) of (3), we would prove directly that the origin of (9a)–(9c) is asymptotically, exponentially stable. As a consequence, all transverse Lyapunov exponents of (3) are negative.

In view of (9a), it is apparent that the more negative the matrix measures (see the definition and the properties in the appendix) of $\bar{\mathbf{G}}$ and $\bar{\mathbf{D}}$ are, the easier the origin of the system (9a)–(9c) is to be made asymptotically stable. However, the choice of a coordinate transformation [25] will greatly influence how negative the matrix measure of $\bar{\mathbf{G}}$ and $\bar{\mathbf{D}}$ could be. In the earlier works, the choice of coordinate transformations is either

$$\mathbf{E}_1 = \begin{pmatrix} 1 & -1 & 0 & \cdots & 0 \\ 1 & 0 & -1 & \ddots & \vdots \\ \vdots & \vdots & \ddots & \ddots & 0 \\ 1 & \cdots & \cdots & 0 & -1 \end{pmatrix}_{(n-1)\times n}$$

or

$$\mathbf{E}_2 = \begin{pmatrix} 1 & -1 & 0 & \cdots & 0 \\ 0 & 1 & -1 & \ddots & \vdots \\ \vdots & \ddots & \ddots & \ddots & 0 \\ 0 & \cdots & 0 & 1 & -1 \end{pmatrix}_{(n-1)\times n.}$$

Note that both $\mathbf{E}_1$ and $\mathbf{E}_2$ are not in $\mathfrak{D}$.

The drawback for the above choices is that even if $\mathbf{G}$ is the diffusive matrix with periodic boundary conditions, the corresponding matrix measure of $\bar{\mathbf{G}}$ is positive whenever $n > 7$ (see [25, Table I]). If $\mathbf{E} \in \mathfrak{D}$ and $\mathbf{G}$ is symmetric, then the corresponding matrix measure of $\bar{\mathbf{G}}$ stays negative regardless the size of the system. (see [25, Theorem 1]).

Sufficient conditions to obtain the synchronization of coupled HR system (3) are stated precisely in the following.

Theorem 1:

i) Assume $x(t)$ satisfies synchronous equation (5). Let λ_2 be the second largest eigenvalue of coupling matrix $\mathbf{G}$. Let $r_2 = \mu_2(\bar{\mathbf{D}})$, the matrix measure of $\bar{\mathbf{D}}$ with respect to

2-norm. Here $\bar{\mathbf{D}}$ is defined in (8c). Set $\alpha =: -1 - r_2/k$ and

$$h_{kg_s,\alpha}(x) = f'(x) + kg_s\left[-p(x) - (v - x)p'(x)\alpha\right]. \quad (10a)$$

Define

$$\sup_x h_{kg_s,\alpha}(x) =: \begin{cases} (h_\alpha)kg_s & \text{if } kg_s \neq 0, \\ d_1 & \text{if } kg_s = 0, \end{cases} \quad (10b)$$

where h_α is a constant and $d_1 = \max_{x\in\mathbb{R}} f'(x) \approx 2.253$. Let $d = \sup_{x(t)} 10|x(t)| \leq 20$. Then coupled HR system (3) is locally synchronized provided that

$$(-\lambda_2)\sigma + (-h_\alpha)kg_s > 24 > d + b, \text{ for } kg_s > 0, \text{ and}$$
$$-\lambda_2\sigma > 26.253 > d + b + d_1, \text{ for } kg_s = 0. \quad (10c)$$

ii) Assume that $\lim_{t\to\infty} x(t) = x_c$. Let $\lim_{t\to\infty} \tilde{\mathbf{H}}(t) := \tilde{\mathbf{H}}_c$. Here $\tilde{\mathbf{H}}(t)$ is defined in (9a). Then system (3) is locally synchronized if all real parts of eigenvalues of

$$\begin{pmatrix} \tilde{\mathbf{H}}_c & \mathbf{I} & -\mathbf{I} \\ -10x_c\mathbf{I} & -\mathbf{I} & \mathbf{0} \\ \mu b\mathbf{I} & \mathbf{0} & -\mu\mathbf{I} \end{pmatrix} =: \bar{\mathbf{H}}_c$$

are negative.

Proof of Theorem 1: To obtain local synchronization of (3), we study (9a)–(9c). Note that for excitatory HR neurons, $x(t) < v = 2$ for all t. Clearly, $\mu_2(\tilde{\mathbf{H}}(t)) \leq \lambda_2\sigma + h_\alpha kg_s =: \lambda$. Here h_α is defined in (10b). Then by Theorem 2 in the appendix,

$$\|\tilde{\mathbf{x}}(t)\| \leq \|\tilde{\mathbf{x}}_0\|e^{\lambda t} + \int_0^t e^{\lambda(t-s)}(\|\tilde{\mathbf{y}}(s)\| + \|\tilde{\mathbf{z}}(s)\|)ds. \quad (11a)$$

Moreover

$$\|\tilde{\mathbf{y}}(t)\| \leq \|\tilde{\mathbf{y}}_0\|e^{-t} + \int_0^t e^{-(t-s)}(d\|\tilde{\mathbf{x}}(s)\|)ds, \quad (11b)$$

and

$$\|\tilde{\mathbf{z}}(t)\| \leq \|\tilde{\mathbf{z}}_0\|e^{-\mu t} + \int_0^t e^{-\mu(t-s)}(\mu b\|\tilde{\mathbf{x}}(s)\|)ds. \quad (11c)$$

Applying Proposition 2-(ii), we see that the first part of the assertion of the theorem holds true provided the real parts of the eigenvalues of

$$\mathbf{B} = \begin{pmatrix} \lambda & 1 & 1 \\ d & -1 & 0 \\ \mu b & 0 & -\mu \end{pmatrix} \quad (12)$$

are negative. Indeed, the Routh-Hurwitz Criterion asserts that it occurs whenever $-\lambda > d + b$. So the first assertion of the Theorem holds true.

The last assertion of the Theorem is a direct consequence of Proposition 3. ∎

If the steady-state synchronization is considered, then some easier verifiable conditions than those stated in Theorem 1-(ii) can be obtained.

Corollary 1: Let $\sigma = 0$. Assume $\lim_{t\to\infty} x(t) = x_c$. Then system (3) without electrical coupling is locally synchronized if the real parts of the eigenvalues of $\bar{\mathbf{A}}$ are negative, where

$$\bar{\mathbf{A}} = \begin{pmatrix} h_{kg_s,-1}(x_c) & 1 & -1 \\ -10x_c & -1 & 0 \\ \mu b & 0 & -\mu \end{pmatrix}. \quad (13)$$

Proof of Corollary 1: Note that $\bar{\mathbf{H}}_c$ with $\sigma = 0$ has the following form:

$$\begin{pmatrix} f'(x_c) + kg_s\left[-p(x_c) + (v - x_c)p'(x_c)\right] & 1 & -1 \\ -10x_c & -1 & 0 \\ \mu b & 0 & -\mu \end{pmatrix}$$
$$\otimes\mathbf{I}_{n-1} + \begin{pmatrix} \mathbf{I}_1 & \mathbf{0} \\ \mathbf{0} & \mathbf{0} \end{pmatrix} \otimes (g_s(v - x_c)p'(x_c)\bar{\mathbf{D}}).$$

Applying Proposition 4, we have that system (3) is locally synchronized provided that

$$\begin{pmatrix} \gamma & 1 & -1 \\ -10x_c & -1 & 0 \\ \mu b & 0 & -\mu \end{pmatrix},$$

where $\gamma = f'(x_c) + kg_s\left[-p(x_c) + (v - x_c)p'(x_c)\right] + g_s(v - x_c)p'(x_c)\bar{\lambda}_i$ and $\bar{\lambda}_i \in \sigma(\bar{\mathbf{D}})$, have all its eigenvalues with negative real parts.

Define matrix $\mathbf{A}(x)$ as

$$\mathbf{A}(x) = \begin{pmatrix} f'(x_c) + x & 1 & -1 \\ -10x_c & -1 & 0 \\ \mu b & 0 & -\mu \end{pmatrix}.$$

Then it can be proved by applying the Routh-Hurwitz Criterion that for any $y < x \leq 0$, if all eigenvalues of $\mathbf{A}(x)$ have positive real parts, then so do those of $\mathbf{A}(y)$.

Upon using the above observation and the fact that $\bar{\lambda}_i$, the real parts of eigenvalues of $\bar{\mathbf{D}}$, are negative, we conclude that the assertion of the Corollary holds true. ∎

Corollary 2: Let $\mathbf{C}$ be a node-balancing matrix, i.e., its row sums and column sums are equal. Assume $\lim_{t\to\infty} x(t) = x_c$. Then system (3) is locally synchronized if all real parts of the eigenvalues of $\bar{\mathbf{A}}$, as given in (13), are negative.

Proof of Corollary 2: As in the proof of Corollary 1, it suffices to show that all real parts of the eigenvalues of $\sigma\bar{\mathbf{G}} + g_s(v - x_c)p'(x_c)\bar{\mathbf{D}}$ are negative. However, by Theorem 2, we have $\lambda_{\max}(\sigma\bar{\mathbf{G}} + g_s(v - x_c)p'(x_c)\bar{\mathbf{D}}) \leq \mu_2(\sigma\bar{\mathbf{G}} + g_s(v - x_c)p'(x_c)\bar{\mathbf{D}}) \leq \sigma\mu_2(\bar{\mathbf{G}}) + g_s(v - x_c)p'(x_c)\mu_2(\bar{\mathbf{D}}) < 0$. Thus, the proof of the Corollary is completed. ∎

Remark 1:
 i) To acquire synchronization of coupled networks, the second largest eigenvalue of the coupling matrix plays an inescapable and decisive role. Indeed, in certain cases, such as the system is fully coupled, the necessary and sufficient condition [26] with $k = 0$ for local synchronization is

$$L_{\max} + \sigma\lambda_2 < 0.$$

Here $L_{\max}$ is the largest Lyapunov exponent of the individual oscillator. In most of interesting networks, λ_2 becomes closer to the origin from the left as the number of oscillators grows. Hence, it takes greater coupling strengths to synchronize the larger system. In other cases, such as the coupled map lattices, the system exhibits the size instability phenomena, that is, the system with the number of nodes greater than a certain critical value loses its synchrony regardless how strong the coupling strength is. Such size instability is induced by the competition between a certain eigenvalues, including λ_2, of the coupling matrix (see [27]). We shall discuss some known upper bounds for λ_2 in Section IV.

ii) If the connection $\mathbf{C}$ is symmetric, then r_2 is the second largest eigenvalue of $\mathbf{D}$. It is easy to see that if the connection network is all-to-all coupled, then $k = n - 1$, $r_2 = -n$ and so $\alpha < 1$. It can be computed that the denser the network is coupled, the larger α is. Hence, α is an indicator of how densely coupled the system is. Note also that $-1 < \alpha \leq 1$. We shall call α the *density* of the coupling network.

To conclude this section, we remark on other existing methods for acquiring synchronization of coupled oscillator systems. The methods include but not limited to the master stability function (MSF), Lyapunov function-based criteria, the matrix measure approach and the partial contraction theory. We refer to [25] for a discussion of our method with the first three approaches described above. We next address the similarity and difference of our approach here and those obtained in [25], [28]. We have made use of the coordinate transformation, which was originated in our earlier work [25], to set up equations. In [25], an iteration scheme was developed to show the origin of the corresponding (9a)–(9c) is asymptotically stable. In this work, we introduce a monotone dynamic approach to show that the system is asymptotically stable, which simplifies the proof substantially. The partial contraction theory [28] is a powerful yet general method to study global synchronization. And its relationship with MSF is addressed in [29]. In the language of authors [28], the main limitation of the method is that the construction of the auxiliary (virtual) system is not systematic. Instead of constructing an auxiliary system, our approach is to apply the contraction theory to (9a)–(9c) directly. Moreover, rather than showing the system to be contracting, which requires its corresponding Jacobian matrix to have a negative matrix measure for all time $t \geq 0$, our approach also differs in the following sense. First, we explore the structure of the Jacobian matrix to give a finer analysis for which the resulting matrix measure is negative. Second, we also examine the possibility of weakening the contracting assumption on the Jacobian matrix by using Proposition 1 in the appendix.

We also mention that the computation cost to verify the synchronous conditions (10c) or (13) is very little as compared to that of computing second Lyapunov exponent of the network. Specifically, if HR system (3) is both electrically and chemically coupled, one needs to check the inequality (10c) to see if the system is synchronized. To check the steady-state synchronization, one only needs to verify the sign of the largest real part

of eigenvalues of a 3×3 matrix, $\bar{\mathbf{A}}$, see (13), regardless of the number of neurons.

IV. MAIN RESULTS

In the section, we shall focus on applying Theorem 1 and Corollaries 1, 2 to coupled HR neurons (3) to extract more detailed synchronization phenomena. To this end, we need to know the dynamics on synchronous manifold.

i) **Dynamics on synchronous manifold** We begin with the study of the dynamics of synchronous equation (5). Its dynamics is to be provided numerically. For $q = 4$, $a = 2.6$, $x_0 = -1.6$, $\mu = 0.01$, $b = 4$, and $v = 2$, the single HR neuron model, i.e., $g_s = 0$, is capable of producing major neuronal behavior, bursting (see, e.g., [17]). Furthermore, such neuron is excitatory, i.e., $x(t) < v = 2$ for all $t \geq 0$. We shall treat kg_s as a bifurcation parameter. The corresponding dynamical behavior of (5) is summarized in Table I. A similar result to Table I was also reported in Fig. 2 of [21]. On the synchronous manifold, the solution trajectory $x(t)$ of (5), depending on initial conditions and kg_s, may settle into various stable states. Fig. 1 provides the maximum Lyapunov exponent (MLE) of synchronous equation (5) versus kg_s. For $0 \leq kg_s \leq 0.85$, there is a set of initial conditions with positive measure for which their corresponding MLE is positive. However, for $0.809 \leq kg_s \leq 0.85$, there is also a set of initial conditions with positive measure for which its corresponding MLE is negative. For instance, if $0.809 \leq kg_s \leq 0.813$, then there are sets of initial conditions with positive measure so that the solution trajectories of (5) converge to a stable periodic solution (see Fig. 2) and stable regular bursting (see Fig. 3), respectively. Specifically, let (x_c, y_c, z_c) be the steady state of (5) (see, Fig. 4), and let

$$C_r = \{(x, y, z) : |x - x_c| < r, |y - y_c| < r, \text{ and } |z - z_c| < r\},$$
(14a)

and

$$I_r = \{(x, y, z) : |x - x_c| > r, |y - y_c| > r, \text{ and } |z - z_c| > r\}.$$
(14b)

In fact, our numerical results suggest that the following hold. Pick, for instance, $kg_s = 0.812$. If the initial condition (x_0, y_0, z_0) is randomly chosen from $C_{0.02}$ (resp., I_1), then its trajectory converges to a periodic orbit (resp., a stable regular bursting) (see Figs. 2 and 3). Similarly, for $kg_s \in [0.814, 0.85]$, synchronous equation (5) also exhibits rich dynamics showing the coexistence of stable multistates. Moreover, if $kg_s \geq 0.814$, the numerical results suggest that the corresponding steady state is locally stable. In fact, a direct calculation shows that a Hopf bifurcation occurs near 0.813. Furthermore, if one performs the linearized stability at the steady-state (x_c, y_c, z_c), then one sees that (x_c, y_c, z_c) is stable whenever $kg_s \geq 0.814$ (see Fig. 5). Such analysis of linearized stability provided some supportive evidence for the validity of Table I.

In summary, the numerical results suggest that on the synchronous manifold, for kg_s small, the regular bursting behavior of single HR persists. For kg_s in an intermediate range, the multistability of (5) occurs. Depending on initial conditions, the coexistence of multistability states including a stable regular
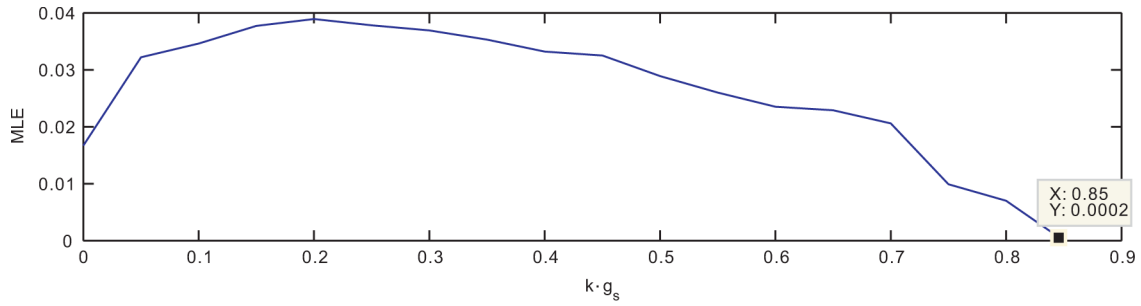
Fig. 1. The maximum Lyapunov exponent (MLE) of synchronous equation (5) is computed for various kg_s. For $0 \leq kg_s \leq 0.85$, MLE > 0 for a set of initial conditions with positive measure. For $kg_s \in [0.809, 0.85]$, there is also a set of initial conditions for which its corresponding MLE < 0.
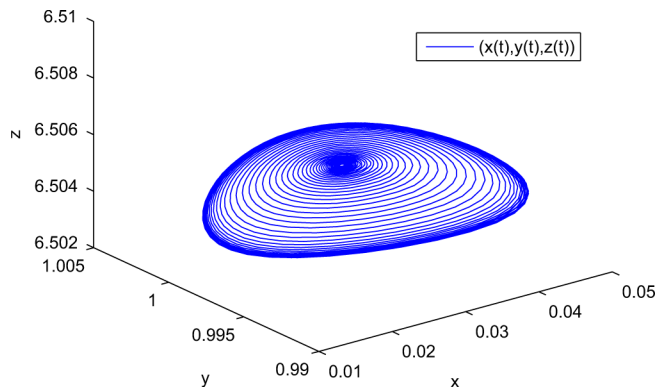

Fig. 2. The solution trajectory with randomly chosen initial conditions from $C_{0.02}$ converges to a stable periodic orbit. Here $kg_s = 0.812$.
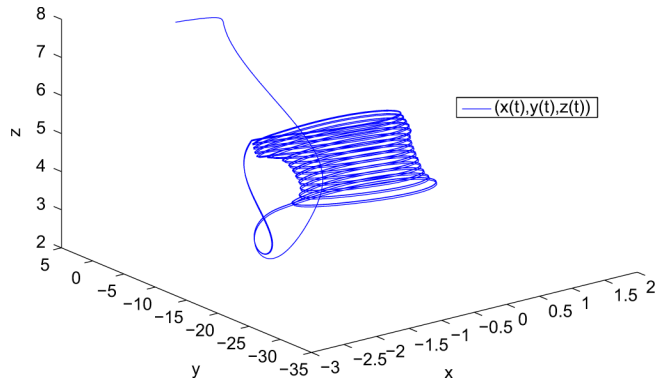

Fig. 3. The solution trajectory with randomly chosen initial conditions from I_1 converges to a stable regular bursting. Here $kg_s = 0.812$.

Fig. 4. Fixed points (x_c, y_c, z_c) for different values kg_s. The fixed point (x_c, y_c, z_c) tends to $(2, -19, 14.4)$ as kg_s tends to infinity.

Fig. 5. The maximum eigenvalue of the linearized operator with respect to the synchronous equation (5) is computed for various kg_s.

bursting and a stable periodic solution/a stable fixed point could be observed. When kg_s becomes large, (5) has a globally asymptotically stable fixed point. Such complex dynamical behavior of synchronous equation (5) leads to the possibility of stable multistate synchronization of coupled HR neurons (3). If the initial conditions and the range of kg_s are so chosen that the corresponding synchronous equation leads to a regular bursting solution, then the associated coupled HR neurons (3) achieves stable regular bursting synchronization. Likewise, we define stable periodic synchronization and stable steady-state synchronization accordingly. As we can see, via Table I, that for $0.809 \leq kg_s \leq 0.85$, the coexistence of stable multistate synchronization of coupled HR neurons (3) could be observed. It should also be mention that the theory of weakly coupled oscilla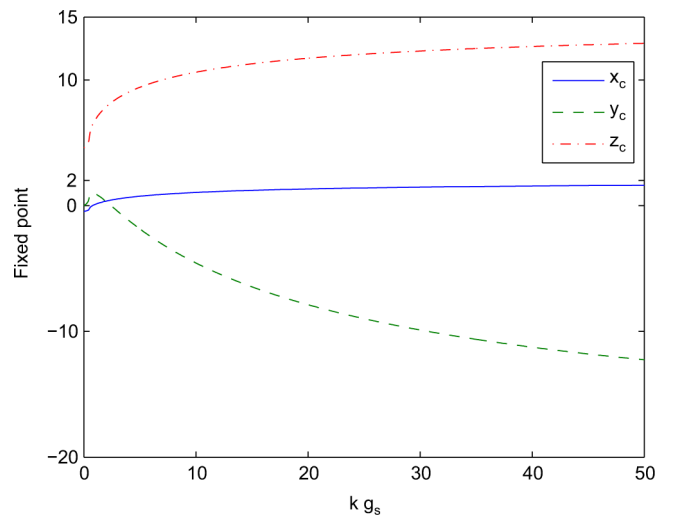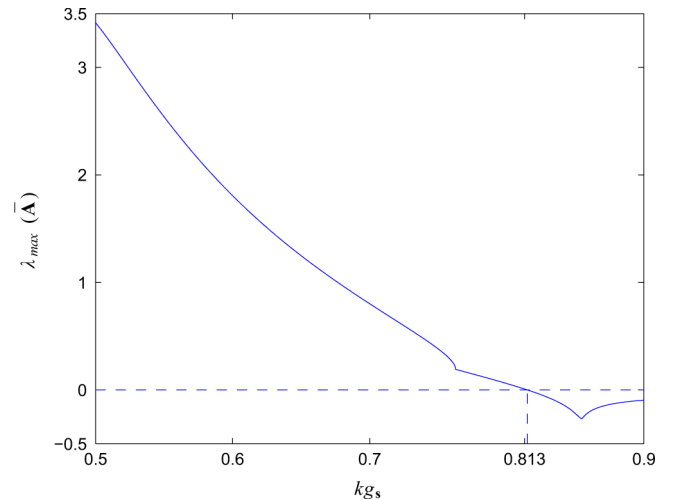tors has often been used to analyze networks of neuron coupled by small chemical synapses g_s, see, e.g., [30], and the many related work cited therein. Using this theory enables one to obtain some extensive analytical insight. Furthermore, the ups and downs of synaptic strength can be controlled. For instant, N-methyl-aspartate receptors can both boost and dampen synaptic efficiency in the brain [31]. Such observations give the justification for the consideration of small chemical synapses g_s.
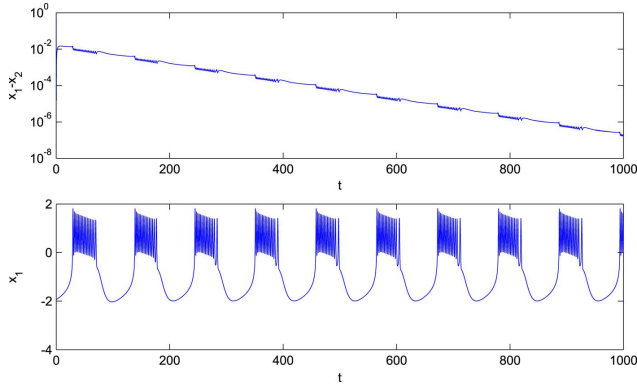
Fig. 6. The time series of $x_1(t) - x_2(t)$ and $x_1(t)$. The graphs demonstrate the stable regular bursting synchronization. Here $g_s = 0.85$, initial $= [-2, -18, 3, -2.5, -18.5, 2.5]$.
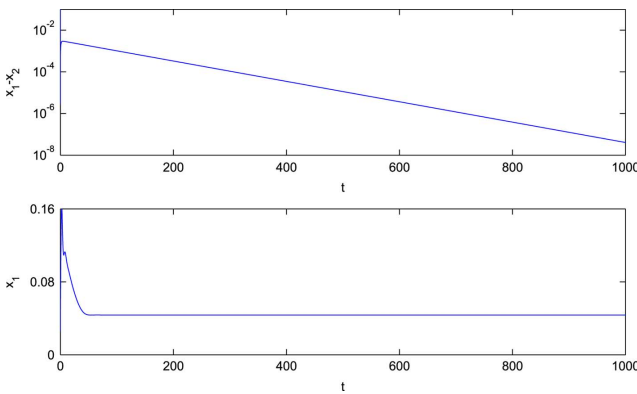

Fig. 7. The time series of $x_1(t) - x_2(t)$ and $x_1(t)$. The graphs demonstrate the stable steady-state synchronization. Here $g_s = 0.85$, initial $= [0.026, 1, 6.5, 0.126, 1.1, 6.6]$.

A. Neurons With Only Chemical Synapse

In [20], a local steady-state synchronization of bursting neurons with no electrical coupling is studied without providing mathematical details. Moreover, their approach fails to see if synchronization of neurons can be achieved when the networks are intermediately and sparsely coupled. Their major contribution was to prove that the bound for achieving synchronization of HR neurons depends only on the number k of chemical signals each neuron receives, and is independent of all other details of the network topology. From (10a) and (10c), it is clear that the larger the density α of the network is, the greater chance coupled HR neurons (3) gets synchronized. In the following, we shall prove that the system of coupled HR neurons (3) achieves steady-state synchronization regardless how sparsely the network is coupled provided that $kg_s \geq 0.87$.

By Corollary 1, it suffices to show that the maximum real part $\lambda_{\max}(\bar{\mathbf{A}})$ of eigenvalue of matrix $\bar{\mathbf{A}}$ defined in (13) is negative. From Fig. 5, we see that $\lambda_{\max}(\bar{\mathbf{A}}) < 0$ whenever $kg_s \geq 0.814$. Upon taking into consideration of the dynamics on synchronous manifold as provided in Table I, we have the following conclusion.

Coupled HR neurons (3) with $\sigma = 0$ achieves the steady-state synchronization for a set of initial conditions with positive measure whenever $kg_s \geq 0.814$ regardless how sparsely the network is coupled, which improves the result obtained in [20]. Moreover, the system acquires the steady-state local synchro-

nization for all initial conditions sufficiently close to each other whenever $kg_s \geq 0.87$.

Numerically, the following scenarios are also observed. Coupled two HR neurons achieves synchronization only when $kg_s \geq 0.809$. Stable regular bursting and steady-state synchronization is found on a set of initial conditions with positive measure, respectively, whenever $kg_s \approx 0.85$. Such numerical results are illustrated in Figs. 6 and 7.

B. Neural Synchronization With Only Electrical Synapse

For $g_s = 0$, by Theorem 1, we obtain stable regular bursting synchronization whenever $\sigma > d + b + d_1/-\lambda_2 =: \sigma_{\min}$. Consider, for instance, a ring of $2l$-nearest-neighbor mutually coupled networks, the predicted minimum electrical coupling strength $\sigma_{\min}$ is computed with the number n of neurons and l being given. Note that in such case

$$\lambda_2 = -4 \sum_{i=1}^{l} \sin^2 \frac{i\pi}{n}$$
$$= \frac{\sin\left((l + \frac{1}{2})\frac{2\pi}{n}\right) - \sin\frac{\pi}{n}}{\sin\frac{\pi}{n}} - 2l. \tag{15a}$$

The results are listed in Table II. For instance, given a number of $(10^4 + 1)$ neurons, it takes the electrical coupling strength 6.66×10^7 or greater to reach synchrony for a network with the nearest-neighbor coupling. It only takes 2.7×10^{-3} or greater to do so for an all-to-all network. If the coupling matrix $\mathbf{G}$ is of high dimension and without fine structure for computers to be able to calculate its second largest eigenvalue effectively, one may use some known estimates to find the upper bound of λ_2. For instance, we have that (see, e.g., [32])

$$\lambda_2 \leq \frac{-2}{(n-1)\bar{\rho}(\mathbf{G}) - \frac{n-2}{2}}, \tag{15b}$$

where $\bar{\rho}(\mathbf{G})$ is the mean distance of the graph associated with $\mathbf{G}$. Upper bounds for $\sigma_{\min}$ by using (15b) are listed in the Table II, too. For $n = 10^4 + 1$, the upper bounds of $\sigma_{\min}$ are 3.29×10^8 and $65\,640$, respectively, for a network with the nearest-neighbor coupling and all-to-all coupling. In a nutshell, connecting each neuron to more neighbors is an effective way for large-size networks to lower the synchronization threshold.

The upper bound for λ_2 in (15b) is quite good for the sparsely coupled networks. Indeed, in the case of the nearest-neighbor coupling, the exact value of λ_2 and its estimated upper are both $O(1/n^2)$. On the other hand, if the network is densely coupled, the upper bound in (15b) gives a poor estimate for λ_2. Nevertheless, if one picks other type of upper bound for λ_2, better estimates could be expected. For example, it is also known, see, e.g., [33], that

$$\lambda_2 \leq -\frac{n}{\beta}, \tag{15c}$$

where $\beta > 0$ is such that $\beta\mathbf{G} + \mathbf{L}$ is negative semidefinite. Here $\mathbf{L}$ is the Laplacian matrix of the complete graph, i.e., $\mathbf{L} = n(\mathbf{I} - \mathbf{ee}^T)$, where $\mathbf{e}$ is given as in (8b). For the all-to-all coupling, it is readily verified that $\beta\mathbf{G} + \mathbf{L}$ with $\beta = 1$ is negative semidefinite. Consequently, the equality in (15c) can be achieved, which yields the best possible estimate.

TABLE II

THE FIRST COMPONENT OF THE PAIR GIVES THE PREDICTED MINIMUM ELECTRICAL COUPLING STRENGTH $\sigma_{\min}$ BY USING THE EXACT VALUE OF λ_2. FOR INSTANCE, WITH $n = 10^2 + 1$, $l = [(n-1)/4] = 25$, THE PREDICTED MINIMUM ELECTRICAL COUPLING STRENGTH IS $\sigma_{\min} = 1.4$. THE SECOND COMPONENT OF THE PAIR IS THE UPPER BOUND OF $\sigma_{\min}$ BY USING (15b)

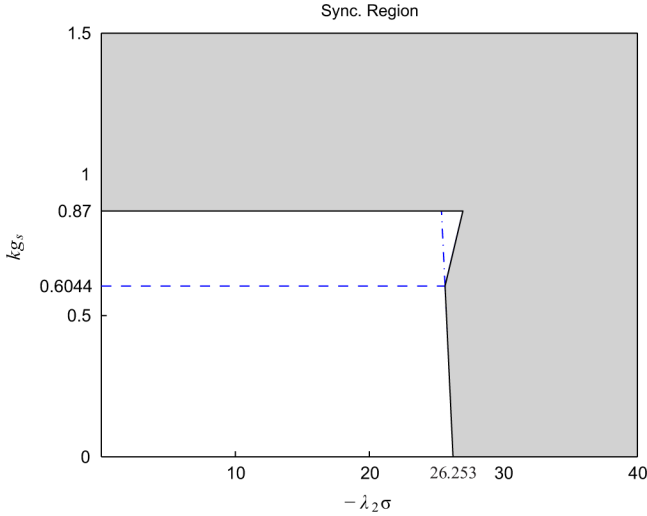| n	21	$10^2 + 1$	$10^3 + 1$	$10^4 + 1$
$l = 1$ (the nearest-neighbor coupling)	$(296, 1320)$	$(6786, 32824)$	$(6.67 \times 10^5, 3.29 \times 10^6)$	$(6.66 \times 10^7, 3.29 \times 10^8)$
$l = [\frac{n-1}{4}]$	$(6.10, 269)$	$(1.40, 1320)$	$(0.1440, 13134)$	$(0.0145, 1.32 \times 10^5)$
$l = \frac{n-1}{2}$ (the all-to-all coupling)	$(1.26, 138)$	$(0.27, 663)$	$(0.0262, 6570)$	$(0.0027, 65640)$

Fig. 8. The shaded area is the synchronization region satisfied by (16) and $kg_s \geq 0.87$.

C. Neural Synchronization With Both Excitatory Chemical and Electrical Synapses

In this subsection, networks with both excitatory electrical and chemical connections are considered. To extract more information on synchronization of the system, we further assume $\mathbf{C}$ to be a node-balancing matrix. We first observe that $x(t) < v$ and $p'(x(t)) \geq 0$ for all t. So h_α, defined in (10b), is decreasing in α. If

$$(-\lambda_2)\sigma + (-h_{-1})kg_s > 24, \tag{16}$$

then (10c) is also satisfied. The synchronization region satisfying (16) and $kg_s \geq 0.87$ is demonstrated in Fig. 8. That is to say, if $(-\lambda_2\sigma, kg_s)$ is chosen from the shaded region in Fig. 8, then multistate or single-state synchronization can be realized depending on the range of kg_s. Consider, for instance, coupled two HR neurons. Let $kg_s = 0.812$ and $\sigma = 30$. If $(x_i(0), y_i(0), z_i(0)) \in C_{0.02}$ (resp., I_1), $i = 1, 2$, as given in (14a) [resp.,(14b)], and are distinct, then the stable periodic (resp., stable regular bursting) synchronization occurs (see Figs. 9 and 10).

We further observe that there exists a t_1 such that $h_{-1} < 0$ (resp., $h_{-1} > 0$) whenever $kg_s \in [0, t_1) =: J_1$ (resp., $kg_s \in (t_1, 0.87] =: J_2$) (see Fig. 8). Here $t_1 \approx 0.6044$. Hence, both chemical and electrical synapses enforce the synchronization phenomena whenever $kg_s \in J_1$. For $kg_s \in J_2$, the chemical synapses play dragging roles for system to reach synchrony. To synchronize, the electrical synapses have to be strong enough to suppress the dragging force created by chemical synapses. Such t_1 is called a *turning point* for h_{-1}.

We are then led to compute turning points for h_α (see Fig. 11). For $\alpha \geq -0.67$ the corresponding turning points are $kg_s = 0.87$. Hence, for $0 \leq kg_s < 0.87$, if the density α of the coupling network is at least -0.67, then chemical synapses can also enforce the synchrony of the system.

To summarize, a synchronization region is obtained in Fig. 8. Particularly, multistate synchronization of coupled HR neurons can be realized whenever $kg_s \in [0.809, 0.85]$ and $(-\lambda_2\sigma, kg_s)$ lies in the synchronization region. Furthermore, for $0 \leq kg_s < 0.87$, if the density α of the coupling network is at least -0.67, then chemical synapses can enforce the synchrony of the system.

To conclude this section, we will elaborate more on some crucial points.

i) As evidence in Table I, the multistable state, which depends on the choice of the initial conditions exist in excitatory HR neuron. In fact, other choice of parameters, such as $a = 3$, $\mu = 0.006$, $q = 3$, $x_0 = -1.56$, $b = 4$, would result the neurons burst irregularly (chaotically). Under such circumstance, the presence of both stable chaotic attractor and stable periodic state can be detected. And our approach can be applied to the above described scenario as well.

ii) From inequality (10c), we see that the denser the coupling network is, or equivalently, the larger the density α is, the easier the system gets synchronized.

iii) We mention that free packages SLEPc developed by V. Hernáendez, J. E. Román, A. Tomás, and V. Vidal [34] can be used to compute λ_2 efficiently.

iv) *In vivo* experiments, the strength of an excitatory mono-synaptic connection has a biologically realistic value $g_s = 0.66 \times 10^{-3}$ (see e.g., [35]). Using such g_s and our theory, we may conclude that if the number of presynaptic neurons that connect to a single cortical neuron is greater than 1319 and in between 1226 and 1288, then the system may reach steady-state synchronization and multistate synchronization, respectively. It should be mentioned that the quantitative description of the circuit of cat area 17 is given in [35]. In cat neocortex, recurrent networks formed between layer $2/3$ pyramidal neurons could form a network that satisfies $kg_s > 0.87$, which could lead to steady-state synchronization. We further consider the combination of three cell classes, pyramidal and basket neurons in layer 4 (p4 and b4), and pyramidal neurons in layer 6 with the preferred layer L5/6 of the axonal innervation (p6(L5/6)). The average number of three presynaptic cell types mentioned above
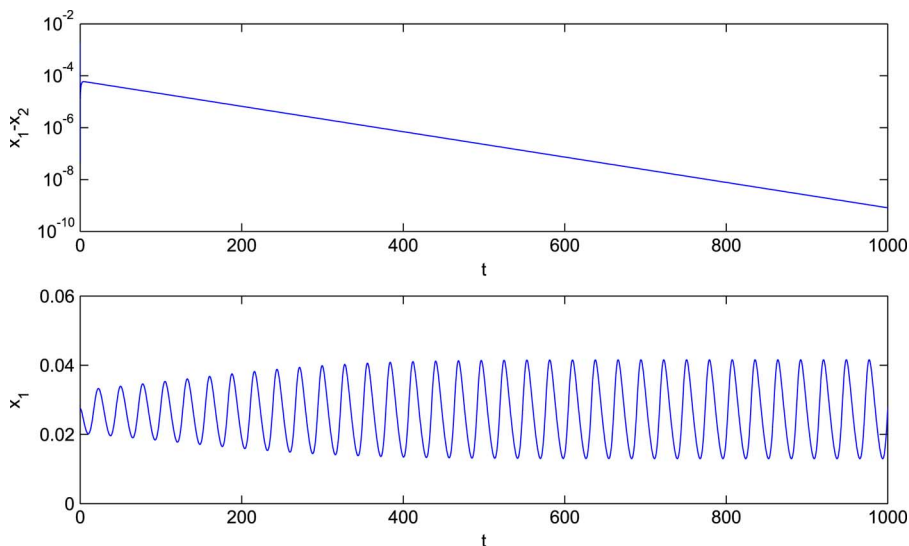
Fig. 9.   The time series of $x_1(t) - x_2(t)$ and $x_1(t)$. The graphs demonstrate the stable periodic synchronization. Here $\sigma = 30, g_s = 0.812$, initial $= \left[0.26459e - 1 + r, 0.996499 + r, 6.5058 + r, 0.26459e - 1 - r, 0.996499 - r, 6.5058 - r \right]$ and $r = 0.001$.
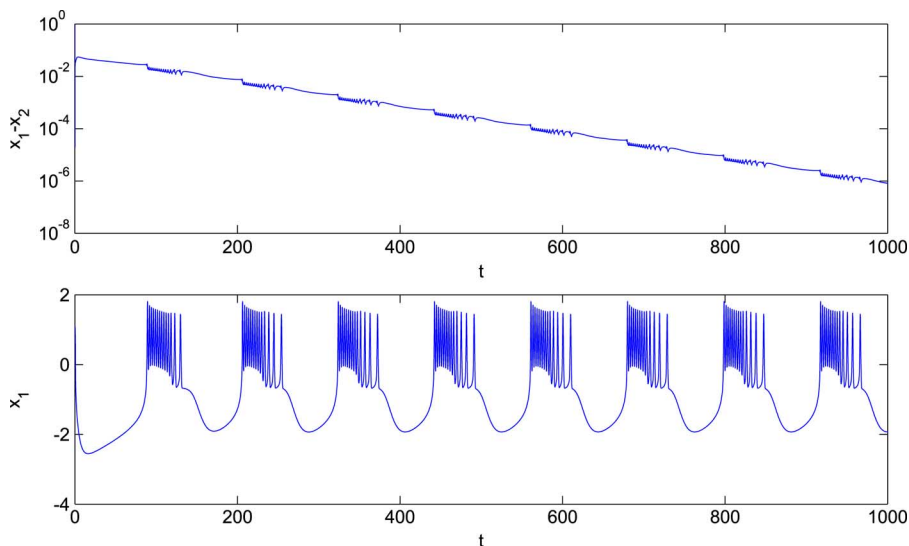

Fig. 10.   The time series of $x_1(t) - x_2(t)$ and $x_1(t)$. The graphs demonstrate the stable regular bursting synchronization. Here $\sigma = 30, g_s = 0.812$, initial $= \left[0.26459e - 1 + r, 0.996499 + r, 6.5058 + r, 0.26459e - 1 - r, 0.996499 - r, 6.5058 - r \right]$ and $r = 1$.

is roughly 1256.4. Our theory then predicts that recurrent networks formed by p4, b4 and p6(L5/6) could lead to multistate synchronization.

V. CONCLUSIONS

Synchronization of coupled HR neurons over complex networks with excitatory chemical and electrical synapses is analytical studied. Particularly, multistate and multistage synchronization is observed with the presence of both chemical and electrical synapses. A measurement for the density of the network is introduced to ensure that chemical synapses play positive effects on the synchronization of the system of coupled neurons. We conclude this work by mentioning the possible future work. It would be interesting to analytically study the rich dynamical behavior of synchronous equation (5). Numerically, one sees that coupled HR neurons are capable of producing multistage synchronization even without the help of electrical
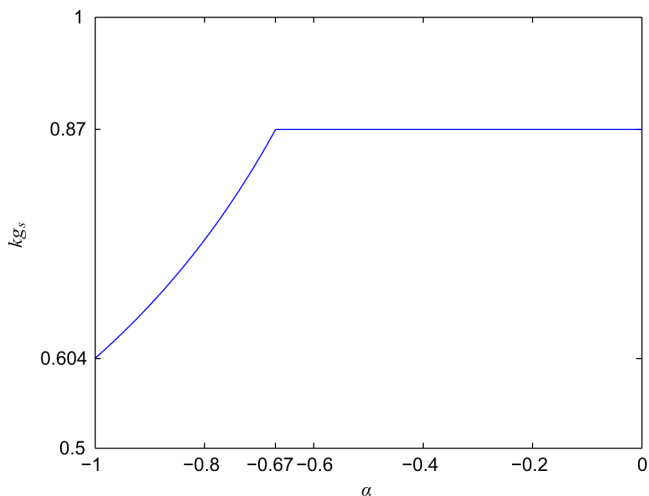

Fig. 11.   Turning points of h_α.

synapses. It is worthwhile to give a rigorous proof. It should also be worthwhile to study HR neurons with inhibitory chemical and electrical synapses. Our numerical work seems to suggest that such system would exhibit the multistage synchronization while the multistate synchronization is lost.

APPENDIX

Definition 1 [36]: Let $\|\cdot\|_i$ be an induced matrix norm on $\mathbb{R}^{n \times n}$. The matrix measure of matrix $\mathbf{K}$ on $\mathbb{R}^{n \times n}$ is defined to be $\mu_i(\mathbf{K}) = \lim_{\epsilon \to 0^+} (\|I + \epsilon\mathbf{K}\|_i - 1)/\epsilon$.

Lemma 1 [36]: Let $\|\cdot\|_k$ be an induced k-norm on $\mathbb{R}^{n \times n}$, where $k = 1, 2, \infty$. Then each of matrix measure $\mu_k(\mathbf{K})$, $k = 1, 2, \infty$, of matrix $\mathbf{K} = (k_{ij})$ on $\mathbb{R}^{n \times n}$ is, respectively,

$$\mu_\infty(\mathbf{K}) = \max_i \left\{ k_{ii} + \sum_{j \neq i} |k_{ij}| \right\},$$

$$\mu_1(\mathbf{K}) = \max_j \left\{ k_{jj} + \sum_{i \neq j} |k_{ij}| \right\},$$

and

$$\mu_2(\mathbf{K}) = \lambda_{\max} \frac{(\mathbf{K}^T + \mathbf{K})}{2}.$$

Here $\lambda_{\max}(\mathbf{K})$ is the maximum eigenvalue of $\mathbf{K}$.

Theorem 2 [36]: i) $\mu_i(\alpha\mathbf{A}) = \alpha\,\mu_i(\mathbf{A})$, $\forall\,\alpha \geq 0$; ii) $\mu_i(\mathbf{A} + \mathbf{B}) \leq \mu_i(\mathbf{A}) + \mu_i(\mathbf{B})$.; iii) If λ is an eigenvalue of $\mathbf{A}$, then $Re\lambda \leq \mu(\mathbf{A})$; iv) Consider the differential equation $\dot{\mathbf{x}}(t) = \mathbf{K}(t)\mathbf{x}(t) + \mathbf{v}(t)$, $t \geq 0$, where $\mathbf{x}(t) \in \mathbb{R}^n$, $\mathbf{K}(t) \in \mathbb{R}^{n \times n}$, and $\mathbf{K}(t), \mathbf{v}(t)$ are piecewise-continuous. Let $\|\cdot\|_i$ be a norm on $\mathbb{R}^n$, and $\|\cdot\|_i, \mu_i$ denote, respectively, the corresponding induced norm and matrix measure on $\mathbb{R}^{n \times n}$. Then whenever $t \geq t_0 \geq 0$, we have

$$\|\mathbf{x}(t)\|_i \leq \|\mathbf{x}(t_0)\|_i \exp\left\{ \int_{t_0}^t \mu_i(\mathbf{K}(s))ds \right\}$$
$$+ \int_{t_0}^t \exp\left\{ \int_s^t \mu_i(\mathbf{K}(\tau))d\tau \right\} \|\mathbf{v}(s)\|_i ds.$$

In our derivation of synchronization of system (3), we need a function being of type K, which generates a monotone dynamics, and a Lyapunov order number of the system of linear differential equations. For completeness and ease of the references, we also recall the definitions of the above described concepts and their properties [36]–[38].

Let $\mathbb{R}^n_+ = \{\mathbf{x} = (x_1, x_2, \dots, x_n)^T \in \mathbb{R}^n : x_i \geq 0, i = 1, \dots, n\}$ be the nonnegative cone. Let $\mathbf{a}, \mathbf{b} \in \mathbb{R}^n$. We write $\mathbf{a} \leq \mathbf{b}$ if $\mathbf{b} - \mathbf{a} \in \mathbb{R}^n_+$.

Definition 2: We say that a function $\mathbf{f} = (f_1, \dots, f_n) : D \subset \mathbb{R}^n \to \mathbb{R}^n$ is of type K on D if, for each i, $f_i(\mathbf{a}) \leq f_i(\mathbf{b})$ whenever $\mathbf{a} = (a_1, \dots, a_n)$ and $\mathbf{b} = (b_1, \dots, b_n)$ are in D with $\mathbf{a} \leq \mathbf{b}$ and $a_i = b_i$.

The following theorem amounts to saying that a vector field being of type K is a sufficient condition to generate a monotone dynamics.

Theorem 3 [38]: Let $\mathbf{f}(t, \mathbf{x})$ be of type K on $\mathbb{R}^n$ for each fixed t and let $\mathbf{x}(t)$ be a solution of $\dot{\mathbf{x}}(t) = \mathbf{f}(t, \mathbf{x})$ on $[a, b]$. Let $\mathbf{z}(t)$ be continuous on $[a, b]$ and satisfy $D_l\mathbf{z}(t) \leq \mathbf{f}(t, \mathbf{z})$. Here

$D_l\mathbf{x}(t) = \lim_{h \to 0^-} [\mathbf{x}(t + h) - \mathbf{x}(t)]/h$. Then $\mathbf{z}(t) \leq \mathbf{x}(t)$ for $a \leq t \leq b$ provided that $\mathbf{z}(a) \leq \mathbf{x}(a)$.

Consider a function $\mathbf{y}(t)$ for $t \geq 0$. A number τ is called a Lyapunov order number [37] for $\mathbf{y}(t)$ if, for every $\epsilon > 0$, there exist positive constants $c_{1,\epsilon}$ and $c_{2,\epsilon}$ such that

$$\|\mathbf{y}(t)\| \leq c_{1,\epsilon} e^{(\tau+\epsilon)t} \text{ for all large } t,$$
$$\|\mathbf{y}(t)\| \geq c_{2,\epsilon} e^{(\tau-\epsilon)t} \text{ for some arbitrary large } t.$$

Consider linear system of differential equations in the homogeneous case

$$\mathbf{y}' = \mathbf{A}(t)\mathbf{y}. \tag{17}$$

Here $\mathbf{A}(t)$ is a $d \times d$ matrix. Clearly, the nontrivial solutions of (17) have d Lyapunov order numbers $\tau_1, \dots, \tau_d$. Let $\tau_{\max} = \max\{\tau_1, \dots, \tau_d\}$. Then $\tau_{\max}$ is called the Lyapunov order number of the system.

Proposition 1 [37]: (i) If $\mathbf{y}(t) \neq 0$ for all large t, then the Lyapunov order number for $\mathbf{y}(t)$ is equal to $\overline{\lim}_{t \to \infty} \ln\|\mathbf{y}(t)\|/t$.

(ii) If $\mathbf{A}(t)$ is continuous for $t \geq 0$, then a sufficient condition for every nontrivial solution $\mathbf{y}(t)$ of (17) to possess an order number τ is that $\int_0^t \|\mathbf{A}(s)\|ds/t$ be bounded, in which case, $\tau \leq \overline{\lim}_{t \to \infty} \int_0^t \mu_2(\mathbf{A}(s))ds/t$.

The following propositions, which, among other things, make use of time average estimates, play critical steps in obtaining our main results.

Proposition 2: i) Suppose $\xi(t)$, $\eta(t)$ and $\zeta(t)$ are nonnegative functions on $[0, \infty)$ satisfying the following inequalities:

$$\xi(t) \leq a_0 \phi_1(t, 0) + \int_0^t \phi_1(t, s)(a_4(s)\eta(s)$$
$$+ a_5(s)\zeta(s))ds, \tag{18a}$$

$$\eta(t) \leq b_0 \phi_2(t, 0) + \int_0^t \phi_2(t, s)(a_6(s)\xi(s)$$
$$+ a_7(s)\zeta(s))ds, \tag{18b}$$

$$\zeta(t) \leq c_0 \phi_3(t, 0) + \int_0^t \phi_3(t, s)(a_8(s)\xi(s)$$
$$+ a_9(s)\eta(s))ds. \tag{18c}$$

Here $a_i(t)$, $i = 4, 5, \dots, 9$, are nonnegative functions on $[0, \infty)$ and $\phi_i(t, s) = e^{\int_s^t a_i(\tau)d\tau}$, $i = 1, 2, 3$. Then $\xi(t)$, $\eta(t)$, and $\zeta(t)$ converge to zero exponentially provided that $\overline{\lim}_{t \to \infty} \int_0^t \mu_2(\mathbf{A}(s))ds/t \leq -r$, for some $r > 0$, where

$$\mathbf{A}(t) = \begin{pmatrix} a_1(t) & a_4(t) & a_5(t) \\ a_6(t) & a_2(t) & a_7(t) \\ a_8(t) & a_9(t) & a_3(t) \end{pmatrix}, \tag{19}$$

ii) Suppose, in addition, that, $a_i(t)$, $i = 1, \dots, 9$, are constants. Then $\xi(t)$, $\eta(t)$, and $\zeta(t)$ converge to zero exponentially provided that all eigenvalues of $\mathbf{A}$ are negative.

Proof: Let $\bar{\xi}(t)$, $\bar{\eta}(t)$ and $\bar{\zeta}(t)$ satisfy the following equation:

$$\dot{\bar{\xi}} = a_1(t)\bar{\xi} + a_4(t)\bar{\eta} + a_5(t)\bar{\zeta}, \bar{\xi}(0) = \xi(0),$$
$$\dot{\bar{\eta}} = a_6(t)\bar{\xi} + a_2(t)\bar{\eta} + a_7(t)\bar{\zeta}, \bar{\eta}(0) = \eta(0),$$
$$\dot{\bar{\zeta}} = a_8(t)\bar{\xi} + a_9(t)\bar{\eta} + a_3(t)\bar{\zeta}, \bar{\zeta}(0) = \zeta(0).$$

It is easily checked that the above system is of type K. It follows from Theorem 3 that $\bar{\xi}(t) \geq \xi(t)$, $\bar{\eta}(t) \geq \eta(t)$, and $\bar{\zeta}(t) \geq \zeta(t)$, for all $t \geq 0$. Using Theorem 3, and Proposition 1-(ii), we see that the first statement of the proposition holds as claimed. The second assertion of the proposition is obvious. ∎

Proposition 3: Let $\dot{\mathbf{x}} = \mathbf{A}(t)\mathbf{x}$. Here $\mathbf{A}(t)$ is an $n \times n$ matrix. Suppose $\lim_{t \to \infty} \mathbf{A}(t) = \bar{\mathbf{A}}$. Then $\mathbf{x}(t)$ converges to the origin exponentially provided that all real parts of eigenvalues of $\bar{\mathbf{A}}$ are negative.

Proof: For any $\epsilon > 0$, there is a $\mathbf{P}_\epsilon$ such that $\bar{\mathbf{A}}$ can be decomposed into a Jordan form of the form, see, e.g., [39, p. 128],

$$\mathbf{P}_\epsilon \bar{\mathbf{A}} \mathbf{P}_\epsilon^{-1} = \mathbf{D} + \epsilon \mathbf{Q},$$

where $\mathbf{D}$ is a diagonal matrix with the diagonal entries being all the eigenvalues of $\bar{\mathbf{A}}$, and $\mathbf{Q}$ is a matrix with its entries being either 0 or 1. Then $\mathbf{P}_\epsilon \mathbf{A}(t) \mathbf{P}_\epsilon^{-1} = \mathbf{P}_\epsilon(\mathbf{A}(t) - \bar{\mathbf{A}})\mathbf{P}_\epsilon^{-1} + \epsilon \mathbf{Q} + \mathbf{D}$. It follows $\mu_2(\mathbf{P}_\epsilon \mathbf{A}(t) \mathbf{P}_\epsilon^{-1}) \leq \mu_2(\mathbf{P}_\epsilon(\mathbf{A}(t) - \bar{\mathbf{A}})\mathbf{P}_\epsilon^{-1}) + \epsilon \mu_2(\mathbf{Q}) + \mu_2(\mathbf{D}) \leq \mu_2(\mathbf{P}_\epsilon(\mathbf{A}(t) - \bar{\mathbf{A}})\mathbf{P}_\epsilon^{-1}) + \epsilon n + \mu_2(\mathbf{D})$. Since $\lim_{t \to \infty} \mathbf{A}(t) = \bar{\mathbf{A}}$, we get

$$\mu_2\left(\mathbf{P}_\epsilon \mathbf{A}(t) \mathbf{P}_\epsilon^{-1}\right) \leq (n+1)\epsilon + \mu_2(\mathbf{D}),$$

whenever $t \geq t_\epsilon$ for some $t_\epsilon > 0$. Hence,

$$\varlimsup_{t \to \infty} \frac{\int_0^t \mu_2\left(\mathbf{P}_\epsilon \mathbf{A}(s) \mathbf{P}_\epsilon^{-1}\right) ds}{t} \leq (n+1)\epsilon + \mu_2(\mathbf{D}).$$

By the arbitrariness of ϵ, take $\epsilon = -\mu_2(\mathbf{D})/2(n+1)$. Then, we have

$$\varlimsup_{t \to \infty} \frac{\int_0^t \mu_2\left(\mathbf{P}_\epsilon \mathbf{A}(s) \mathbf{P}_\epsilon^{-1}\right) ds}{t} \leq \frac{\mu_2(\mathbf{D})}{2}.$$

Thus, all solutions of $\dot{\mathbf{y}} = (\mathbf{P}_\epsilon \mathbf{A}(t) \mathbf{P}_\epsilon^{-1})\mathbf{y}$ converges to the origin, and so are those of $\dot{\mathbf{x}} = \mathbf{A}(t)\mathbf{x}$.

Proposition 4: Let $\mathbf{A}$ and $\mathbf{G}$ be matrices of dimension $m \times m$ and $n \times n$, respectively, and $\mathbf{I}_p$ be the $p \times p$ identity matrix. Let λ_i, $i = 1, \ldots, k$, be all the eigenvalues of $\mathbf{G}$. Then the real parts of the eigenvalues of

$$(\mathbf{A} \otimes \mathbf{I}_n) + \left(\begin{pmatrix} \mathbf{I}_1 & \mathbf{0} \\ \mathbf{0} & \mathbf{0} \end{pmatrix} \otimes \mathbf{G}\right)$$

are negative provided that all real parts of the eigenvalues of matrices

$$\mathbf{M}_i := \mathbf{A} + \lambda_i \begin{pmatrix} \mathbf{I}_1 & \mathbf{0} \\ \mathbf{0} & \mathbf{0} \end{pmatrix}$$

are negative.

Proof: For any $\epsilon > 0$, there is $\mathbf{P}_\epsilon$ such that

$$\mathbf{P}_\epsilon \mathbf{G} \mathbf{P}_\epsilon^{-1} = \mathbf{D} + \epsilon \mathbf{Q},$$

where $\mathbf{D}$ is a diagonal matrix with the diagonal entries being all the eigenvalues of $\mathbf{G}$, and $\mathbf{Q}$ is a matrix with its entries being either 0 or 1. Then

$$\begin{aligned}
(\mathbf{I}_m \otimes \mathbf{P}_\epsilon) &\left[(\mathbf{A} \otimes \mathbf{I}_n) + \left(\begin{pmatrix} \mathbf{I}_1 & \mathbf{0} \\ \mathbf{0} & \mathbf{0} \end{pmatrix} \otimes \mathbf{G}\right)\right] (\mathbf{I}_m \otimes \mathbf{P}_\epsilon^{-1}) \\
&= \left\{(\mathbf{A} \otimes \mathbf{I}_n) + \begin{pmatrix} \mathbf{I}_1 & \mathbf{0} \\ \mathbf{0} & \mathbf{0} \end{pmatrix} \otimes \mathbf{D}\right\} + \epsilon \begin{pmatrix} \mathbf{I}_1 & \mathbf{0} \\ \mathbf{0} & \mathbf{0} \end{pmatrix} \otimes \mathbf{Q}.
\end{aligned}$$

By taking ϵ sufficiently small, we get real parts of the eigenvalues of

$$(\mathbf{A} \otimes \mathbf{I}_n) + \left(\begin{pmatrix} \mathbf{I}_1 & \mathbf{0} \\ \mathbf{0} & \mathbf{0} \end{pmatrix} \otimes \mathbf{G}\right)$$

are negative iff those of

$$(\mathbf{A} \otimes \mathbf{I}_n) + \begin{pmatrix} \mathbf{I}_1 & \mathbf{0} \\ \mathbf{0} & \mathbf{0} \end{pmatrix} \otimes \mathbf{D} \qquad (20)$$

are negative. Then, the proof is completed by noting that after some permutation, matrix in (20) becomes $\mathrm{diag}(\mathbf{W}_1, \ldots, \mathbf{W}_n)$, where $\mathbf{W}_i = \mathbf{M}_j$, for some $j = 1 \ldots, k$. ∎

REFERENCES

[1] Z. Huang, Q. Song, and C. Feng, "Multistability in networks with self-excitation and high-order synaptic connectivity," *IEEE Trans. Circuits Syst. I, Reg. Papers*, vol. 57, no. 8, pp. 2144–2155, Aug. 2010.

[2] S. Hashimoto and H. Torikai, "A novel hybrid spiking neuron: Bifurcations, responses, and on-chip learning," *IEEE Trans. Circuits Syst. I, Reg. Papers*, vol. 57, no. 8, pp. 2168–2181, Aug. 2010.

[3] T. M. Massoud and T. K. Horiuchi, "A neuromorphic VLSI head direction cell system," *IEEE Trans. Circuits Syst. I, Reg. Papers*, vol. 58, no. 1, pp. 150–163, Jan. 2011.

[4] W. Singer, "Neuronal synchrony: A versatile code for the definition of relations?," *Neuron*, vol. 24, no. 1, pp. 49–65, Sep. 1999.

[5] P. J. Uhlhaas and W. Singer, "Neural synchrony in brain disorders: Relevance for cognitive dysfunctions and pathophysiology," *Neuron*, vol. 52, no. 1, pp. 155–168, Oct. 2006.

[6] S. Neuenschwander and W. Singer, "Long-range synchronization of oscillatory light responses in the cat retina and lateral geniculate nucleus," *Nature*, vol. 379, pp. 728–732, 1996.

[7] L. Glass, "Synchronization and rhythmic processes in physiology," *Nature*, vol. 410, no. 6825, pp. 277–284, 2001.

[8] C. M. Gray, P. Konig, A. K. Engel, and W. Singer, "Oscillatory responses in cat visual cortex exhibit inter-columnar synchronization which reflects global stimulus properties," *Nature*, vol. 338, pp. 334–337, 1989.

[9] R. Dzakpasu and M. Zochowski, "Discriminating differing types of synchrony in neural systems," *Phys. D*, vol. 208, no. 1–2, pp. 115–122, 2005.

[10] G. Buzsaki, *Rhythms of the Brain*. New York: Oxford Univ. Press, 2006.

[11] C. J. Stam, B. F. Jones, G. Nolte, M. Breakspear, and S. Ph, "Small-world networks and functional connectivity in alzheimer's disease," *Cereb. Cortex*, vol. 17, no. 1, pp. 92–99, 2006.

[12] G. Innocenti, A. Morelli, R. Genesio, and A. Torcini, "Dynamical phases of the Hindmarsh-Rose neuronal model: Studies of the transition from bursting to spiking chaos," *Chaos*, vol. 17, no. 4, p. 043128, 2007.

[13] E. M. Izhikevich, "Which model to use for cortical spiking neurons?," *IEEE Trans. Neural Netw.*, vol. 15, no. 5, pp. 1063–1070, Sep. 2004.

[14] M. Storace, D. Linaro, and E. de Lange, "The Hindmarsh-Rose neuron model: Bifurcation analysis and piecewise-linear approximations," *Chaos*, vol. 18, no. 3, p. 033128, 2008.

[15] E. de Lange and M. Hasler, "Predicting single spikes and spike patterns with the Hindmarsh-Rose model," *Biol. Cybern.*, vol. 99, no. 4, pp. 349–360, 2008.

[16] J. L. Hindmarsh and R. M. Rose, "A model of neuronal bursting using three coupled first order differential equations," *Proc. R. Soc. Lond. B*, vol. 221, no. 1222, pp. 87–102, 1984.

[17] G. Innocenti and R. Genesio, "On the dynamics of chaotic spiking-bursting transition in the Hindmarsh-Rose neuron," *Chaos*, vol. 19, no. 2, p. 023124, 2009.

[18] M. Jalili, "Synchronizing Hindmarsh-Rose neurons over Newman-Watts networks," *Chaos*, vol. 19, no. 3, p. 033103, 2009.

[19] N. Kopell and B. Ermentrout, "Chemical and electrical synapses perform complementary roles in the synchronization of interneuronal networks," *PNAS*, vol. 101, no. 43, pp. 15482–15487, 2004.

[20] I. V. Belykh, E. de Lange, and M. Hasler, "Synchronization of bursting neurons: What matters in the network topology," *Phys. Rev. Lett.*, vol. 94, no. 18, p. 188101, May 2005.

[21] P. Checco, M. Righero, M. Biey, and L. Kocarev, "Synchronization in networks of Hindmarsh-Rose neurons," *IEEE Trans. Circuits Syst. II, Exp. Briefs*, vol. 55, no. 12, pp. 1274–1278, Dec. 2008.

[22] Q. Y. Wang, Q. S. Lu, G. R. Chen, and D. H. Guo, "Chaos synchronization of coupled neurons with gap junctions," *Phys. Lett. A*, vol. 356, no. 1, pp. 17–25, 2006.

[23] Q. Wang, M. Perc, Z. Duan, and G. Chen, "Synchronization transitions on scale-free neuronal networks due to finite information transmission delays," *Phys. Rev. E*, vol. 80, no. 2, p. 026206, Aug. 2009.

[24] Q. Wang, G. Chen, and M. Perc, "Synchronous bursts on scale-free neuronal networks with attractive and repulsive coupling," *PLoS ONE*, vol. 6, no. 1, p. 15851, 2011.

[25] J. Juang and Y.-H. Liang, "Coordinate transformation and matrix measure approach for synchronization of complex networks," *Chaos*, vol. 19, no. 3, p. 033131, 2009.

[26] S.-F. Shieh, Y. Wang, G.-W. Wei, and C.-H. Lai, "Mathematical proof for wavelet method of chaos control," *J. Math. Phys.*, vol. 47, no. 8, p. 082701, 2006.

[27] J. Juang and Y.-H. Liang, "Synchronous chaos in coupled map lattices with general connectivity topology," *SIAM J. Appl. Dyn. Syst.*, vol. 7, no. 3, pp. 755–765, 2008.

[28] W. Wang and J.-J. E. Slotine, "On partial contraction analysis for coupled nonlinear oscillators," *Biol. Cybernet.*, vol. 92, no. 1, pp. 38–53, 2005.

[29] G. Russo and M. di Bernardo, "Contraction theory and master stability function: Linking two approaches to study synchronization of complex networks," *IEEE Trans. Circuits Syst. II, Exp. Briefs*, vol. 56, no. 2, pp. 177–181, Feb. 2009.

[30] T. J. Lewis and J. Rinzel, "Dynamics of spiking neurons connected by both inhibitory and electrical coupling," *J. Comp. Neurosci.*, vol. 14, pp. 283–309, 2003.

[31] T. Bliss and R. Schoepfer, "Controlling the ups and downs of synaptic strength," *Science*, vol. 304, no. 5673, pp. 973–974, 2004.

[32] B. Mohar, "Eigenvalues, diameter, and mean distance in graphs," *Graphs Combinatorics*, vol. 7, no. 1, pp. 53–64, 1991.

[33] C. W. Wu, *Synchronization in Complex Networks of Nonlinear Dynamical Systems*. Hackensack, NJ: World Scientific, 2007.

[34] V. Hernández, J. E. Román, A. Tomás, and V. Vidal, Krylov-Schur methods in slepc 2007 [Online]. Available: http://www.grycap.upv.es/slepc

[35] T. Binzegger, R. J. Douglas, and K. A. C. Martin, "Topology and dynamics of the canonical circuit of cat V1," *Neural Netw.*, vol. 22, no. 8, pp. 1071–1078, 2009.

[36] M. Vidyasagar, *Nonlinear Systems Analysis*. Englewood Cliffs, NJ: Prentice-Hall, 1978.

[37] P. Hartman, *Ordinary Differential Equations*, ser. Classics in Applied Mathematics, 2nd ed. Philadelphia, PA: Society for Industrial and Applied Mathematics, 2002.

[38] S. B. Hsu, *Ordinary Differential Equations With Applications*, ser. Applied Mathematics. Hackensack, NJ: World Scientific, 2006.

[39] R. A. Horn and C. R. Johnson, *Matrix Analysis*. New York: Cambridge Univ. Press, 1990.

Fang-Jhu Jhou received the B.S. degree in mathematics from National Changhua University of Education, Changhua, Taiwan, in 2005, and the M.S. degree in mathematical modeling and scientific computing from National Chiao Tung University, Hsinchu, Taiwan, in 2010.

Her current research interests include control theory, dynamical systems, chaos theory, and biological networks.

Jonq Juang received the Ph.D. degree in mathematics from Texas Tech University, Lubbock, in 1988.

He is currently a Distinguished Professor with the Department of Applied Mathematics and Center of Mathematics Modeling and Scientific Computing, National Chiao Tung University, Hsinchu, Taiwan. His current research interests include dynamical systems, differential equations, and their applications.

Yu-Hao Liang received the B.S. degree in mathematics from National Taiwan University, Taipei, in 2005, and the M.S. degree and the Ph.D. degree in applied mathematics from National Chiao Tung University, Hsinchu, Taiwan, in 2007, and 2011, respectively. His current research interests include control theory, dynamical systems, chaos theory, and biological networks.